IEEE Access
Multidisciplinary : Rapid Review : Open Access Journal

Received 7 June 2023, accepted 13 July 2023, date of publication 19 July 2023, date of current version 26 July 2023.

Digital Object Identifier 10.1109/ACCESS.2023.3296788

RESEARCH ARTICLE

Random Beam-Based Non-Orthogonal Multiple Access for Massive MIMO Low Earth Orbit Satellite Networks

JUNG HOON LEE[1], (Member, IEEE), JUNG SUK JOO[1], PANSOO KIM[2], AND JOON-GYU RYU[2]

[1]Department of Electronics Engineering and Applied Communications Research Center, Hankuk University of Foreign Studies, Yongin 17035, South Korea
[2]Satellite Communication Research Division, Electronics and Telecommunications Research Institute (ETRI), Daejeon 34129, South Korea

Corresponding author: Pansoo Kim (pskim@etri.re.kr)

This work was supported by the Institute of Information and Communications Technology Planning and Evaluation (IITP) funded by the Korean Government (MSIT) through the Development of 3D Spatial Satellite Communications Technology under Grant 2021-0-00847.

ABSTRACT In this paper, we propose random beam-based non-orthogonal multiple access (NOMA) for massive multiple-input multiple-output (MIMO) low earth orbit (LEO) satellite communication systems that operate with frequency-division duplexing (FDD). Our system model consists of a massive-antenna satellite and multiple single-antenna users within its coverage area. The satellite selectively serves a subset of users based on a target signal-to-interference-plus-noise power ratio (SINR). In the random beam-based NOMA, the satellite utilizes random beams, where each beam can support multiple users using NOMA. To facilitate user selection and power allocation, each user provides several scalar values obtained from statistical channel state information (CSI) as feedback to the satellite. This allows us to reduce the computational complexity of beamforming design and minimize the feedback overhead for channel acquisition. We propose two random beam-based NOMA schemes with varying complexities and feedback overheads. We optimize these schemes by solving joint user selection and power allocation problems. The numerical results demonstrate that our proposed schemes outperform conventional random beamforming, specifically orthogonal multiple access (OMA) at each beam, by supporting a greater number of users.

INDEX TERMS Low earth-orbit (LEO) satellite communications, massive multiple-input multiple-output (MIMO), non-orthogonal multiple access (NOMA), random beamforming.

I. INTRODUCTION

Satellite communications are expected to be one of the promising technologies for expanding the coverage of terrestrial wireless communication systems. In particular, low earth orbit (LEO) satellite communication, operating at orbits below 2000 km, is emerging as a key technology due to its lower power consumption and relatively small propagation delay. Consequently, various projects such as Starlink, OneWeb, SpaceX, Telesat, etc. are currently underway [1], [2]. With the successful evolution of terrestrial communication systems, there have also been significant efforts to enhance the performance of satellite communication systems. Among these efforts, extensive research has been conducted on leveraging a large number of antennas in satellite communication systems.

By employing multiple antennas, a satellite can simultaneously support multiple users using different beams. However, inter-beam interference poses a significant challenge and can severely degrade system performance. To address this issue, the authors of [2] and [3] propose the exclusive use of frequency bands among adjacent beams. Additionally, to increase spectral efficiency, authors in [3], [4], [5], [6], and [7] explore full frequency reuse within each beam, while mitigating inter-beam interference through techniques such as transmitter precoding or receiver postprocessing (e.g., multiuser detection).

In wireless communications, transmitters require channel state information (CSI) to adapt to channel conditions. In time-division duplexing (TDD) systems, transmitters can

The associate editor coordinating the review of this manuscript and approving it for publication was Bilal Khawaja.

directly obtain CSI from the received signal based on uplink/downlink channel reciprocity. However, in frequency-division duplexing (FDD) systems, the uplink and downlink channels are independent, requiring receivers to aid transmitters in CSI acquisition. In satellite communication, the use of instantaneous CSI is nearly impossible due to significant propagation delays. Even in TDD systems, the CSI obtained from the uplink channel is no longer valid for downlink transmission. To overcome this challenge, there have been many research considering exploitation of statistical CSI for satellite communications [8], [9]. The authors of [8] introduced massive multiple-input multiple-output (MIMO) transmission/reception at the satellite based on the statistical CSI. The authors of [9] proposed deep learning-based channel prediction for LEO satellites with massive antennas.

Recent advancements in wireless communication systems have facilitated the emergence of various wireless applications with the increasing number of wireless devices [10]. One way to support a large number of users is non-orthogonal multiple access (NOMA) [11], [12], [13]. In NOMA, multiple users share the same radio resource, unlike conventional orthogonal multiple access (OMA), where each user exclusively occupies wireless resources. In downlink (power-domain) NOMA, a transmitter allocates different powers to serve multiple users. In this case, the transmitter transmits the superposed signals of the users, and each user decodes its own signals through successive interference cancellation (SIC). During this process, a user with a better channel condition can decode the signals of other users with relatively poor channels, allowing for partial subtraction of interference from the received signal. Meanwhile, the transmitter should allocate more power to the user with the worse channel condition.

NOMA has been extensively studied in various scenarios. For instance, in [14], the authors proposed NOMA with an intelligent reflecting surface (IRS) to serve cell edge users. Additionally, [15] and [16] focused on machine learning techniques for implementing NOMA. In a satellite communication system, the authors of [17] introduced a resource allocation scheme for NOMA with multiple beams to satisfy the quality of service (QoS) requirements of each user. The authors of [18] proposed NOMA for multi-user visible light communication systems. Also, the authors of [19] proposed a user selection and power allocation with NOMA in the presence of both geostationary and LEO satellites. In [20], the authors proposed a beamforming design aimed at maximizing the achievable rate in a LEO satellite communication system by taking into account NOMA and massive antenna settings.

In this paper, we propose random beam-based NOMA for massive MIMO LEO satellite communication systems operated with FDD, where each user has a QoS constraint. In our system model, a LEO satellite is equipped with massive antennas, and there are single-antenna users within its coverage area. The satellite selects and serves a subset of these users. As mentioned earlier, satellites face challenges in using instantaneous CSI due to the large propagation delay. Additionally, beamforming design is complicated by the need for channel feedback and computational complexity. To address these issues, we propose two random beam-based NOMA schemes with different complexities and feedback overheads. These schemes leverage random beams and statistical CSI. While prior work on random beam-based NOMA has been presented in [21] considering MIMO broadcast channels, our problem setting differs significantly. In this paper, we focus on massive MIMO satellite communications, necessitating considerations of massive antennas, a LEO channel model, and statistical CSI.

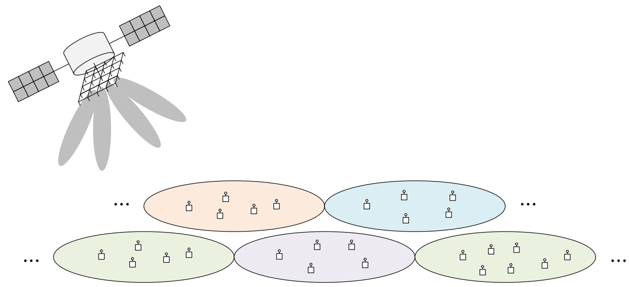

FIGURE 1. System model. A massive-antenna LEO satellite selects and serves some users on the coverage.

Our contributions can be summarized as follows:

- We propose random beam-based NOMA for massive MIMO LEO satellite communication systems. In this scheme, each beam can support multiple users using NOMA.
- We formulate a joint user selection and power optimization problem for random beam-based NOMA under the uniform planar array (UPA) antenna setting, leveraging statistical CSI.
- We propose two random beam-based NOMA schemes with varying computational complexities and feedback overheads. For each scheme, we determine the specific feedback information required from each user.
- To optimize our proposed schemes, we determine the optimal user selection and power allocation for each scheme.
- We evaluate our random beam-based NOMA schemes and demonstrate their ability to effectively exploit multiuser diversity provided by multiple users, resulting in improved performance compared to conventional random beamforming (i.e., OMA at each beam).

The remainder of this paper is organized as follows. In Section II, we explain our system model, and in Section III, we propose random beam-based NOMA. In Section IV, we optimize our proposed schemes, and in Section V, we evaluate our proposed schemes. In Section VI, we conclude our paper.

II. SYSTEM MODEL

Our system model is illustrated in Fig. 1. We consider a downlink of a LEO satellite communication system, where massive antennas are equipped at the satellite. In this case, we assume that the massive antennas are with the form of an $N_x \times N_y$ uniform planar array (UPA), where N_x and N_y are the numbers of antennas on the x-axis and the y-axis, respectively. There are K single-antenna users on the ground in the coverage, and the satellite selects and serves some among them. When the carrier frequency is f_c, the user k's received signal at the time instance t can be modelled by

$$y_k(t, f_c) = \mathbf{h}_k(t, f_c)^\dagger \mathbf{x}(t, f_c) + n_k(t, f_c), \tag{1}$$

where $\mathbf{h}_k(t, f_c) \in \mathbb{C}^{N_x N_y \times 1}$ is a channel vector from the satellite to the user k, and $\mathbf{x}(t, f_c) \in \mathbb{C}^{N_x N_y \times 1}$ is the transmitted signal from the satellite. Also, $n_k(t, f_c) \in \mathbb{C}^{1\times 1}$ is a circularly symmetric complex Gaussian noise at the user k with zero mean and unit variance, i.e., $n_k(t, f_c) \sim \mathcal{CN}(0, 1)$.

In massive MIMO satellite communications, the channel vector $\mathbf{h}_k(t, f_c) \in \mathbb{C}^{N_x N_y \times 1}$ can be decomposed into two terms as follows:

$$\mathbf{h}_k(t, f_c) = \mathbf{h}_k^{\text{LoS}}(t, f_c) + \mathbf{h}_k^{\text{NLoS}}(t, f_c), \tag{2}$$

where $\mathbf{h}_k^{\text{LoS}}(t, f_c) \in \mathbb{C}^{N_x N_y \times 1}$ is a line-of-sight (LoS) component, and $\mathbf{h}_k^{\text{NLoS}}(t, f_c) \in \mathbb{C}^{N_x N_y \times 1}$ is a non-line-of-sight (NLoS) component. Under the UPA antenna setting, the LoS and the NLoS terms can be represented by

$$\begin{aligned}\mathbf{h}_k^{\text{LoS}}(t, f_c) &= \sqrt{\frac{\eta_k}{\eta_k+1}}\xi_k \exp\left(j2\pi(f_k^{\text{D,LoS}} - f_c\tau_k^{\text{LoS}})\right)\\ &\quad \times \mathbf{u}_k(\theta_k^{\text{LoS}}, \psi_k^{\text{LoS}}) \end{aligned}\tag{3}$$

$$\begin{aligned}\mathbf{h}_k^{\text{NLoS}}(t, f_c) &= \sqrt{\frac{1}{\eta_k+1}}\sqrt{\frac{1}{L_k}}\sum_{l=1}^{L_k}\Big[\xi_{k,l} \exp\Big(j2\pi(f_{k,l}^{\text{D,NLoS}}\\ &\quad - f_c\tau_{k,l}^{\text{NLoS}})\Big)\mathbf{u}_k(\theta_{k,l}^{\text{NLoS}}, \psi_{k,l}^{\text{NLoS}})\Big], \end{aligned}\tag{4}$$

where $\eta_k \in [0, 1]$ is the Rician factor, and ξ_k is the complex-valued channel magnitude of the LoS component at user k. Also, in (3), τ_k^{LoS} and $f_k^{\text{D,LoS}}$ are the propagation delay and the relativistic Doppler shift caused by the motions of both the satellite and the user k in the LoS component, respectively. Meanwhile, in (4), L_k is the number of NLoS paths to the user k, and $\xi_{k,l}$ is the complex-valued channel magnitude of the lth NLoS path of the user k, while $\tau_{k,l}^{\text{NLoS}}$ and $f_{k,l}^{\text{D,NLoS}}$ are the propagation delay and the relativistic Doppler shift caused by the motions of both the satellite and the user k in the lth NLoS path, respectively.

In (3) and (4), θ_k^{LoS} and ψ_k^{LoS} denote the angles of the horizontal and the vertical directions of the LoS path, respectively, while $\theta_{k,l}^{\text{NLoS}}$ and $\psi_{k,l}^{\text{NLoS}}$ are the angles of the horizontal and the vertical directions of the lth NLoS path. The notation $\mathbf{u}_k(\theta, \psi)$ is the array response vector to the user k defined by

$$\mathbf{u}_k(\theta, \psi) = \mathbf{u}_{k,x}(\theta, \psi) \otimes \mathbf{u}_{k,y}(\theta, \psi), \tag{5}$$

where $\otimes$ denotes the Kronecker product, while $\mathbf{u}_{k,x}(\theta, \psi)$ and $\mathbf{u}_{k,y}(\theta, \psi)$ are respectively given by

$$\begin{aligned}\mathbf{u}_{k,x}(\theta, \psi) &\triangleq [1, \exp(-j\phi), \ldots, \exp(-j(N_x-1)\phi)]\\ \mathbf{u}_{k,y}(\theta, \psi) &\triangleq [1, \exp(-j\phi), \ldots, \exp(-j(N_y-1)\phi)],\end{aligned}$$

where $\phi \triangleq \frac{2\pi d f_c}{c}\cos\theta \sin\psi$ with antenna spacing d and the speed of light c.

Different from terrestrial wireless communications, in (2), the LoS component is dominant, and the angular spreads of NLoS paths are relatively small. This is because the satellite is far in the high altitude, while the scatters are relatively very close to the user on the ground. Thus, it is quite common to assume that the angles of the NLoS paths are identical to those of the LoS path, i.e., $\theta_{k,1}^{\text{NLoS}} = \ldots = \theta_{k,L_k}^{\text{NLoS}} = \theta_k^{\text{LoS}}$ and $\psi_{k,1}^{\text{NLoS}} = \ldots = \psi_{k,L_k}^{\text{NLoS}} = \psi_k^{\text{LoS}}$. Thus, we can rewrite the channel vector (2) as (6), shown at the bottom of the page.

For notational simplicity, in the latter part of the paper, we omit the time index t and the frequency index f_c in the channel representation, e.g., $\mathbf{h}_k \triangleq \mathbf{h}_k(t, f_c)$, as the channel is mainly dependent on the propagation delay and the Doppler shifts.

To support multiple users, the satellite adopts linear beamforming with M unit vectors $\mathbf{v}_1, \ldots, \mathbf{v}_M \in \mathbb{C}^{N_x N_y \times 1}$ such that $\|\mathbf{v}_1\|^2 = \ldots = \|\mathbf{v}_M\|^2 = 1$. Let $\mathcal{G}_m \in [K]$ be the set of users served by the mth beam simultaneously.[1] Then, the transmitted signal $\mathbf{x}$ in (1) is constructed as follows

$$\mathbf{x} = \sum_{i=1}^{M}\sum_{j\in\mathcal{G}_i}\mathbf{v}_i x_j, \tag{7}$$

where $x_k \in \mathbb{C}^{1\times 1}$ is the transmit symbol to the user k such that $\mathbb{E}|x_k|^2 = P_k$ with P_k the allocated power to the user k. Denoting by P the total transmit power budget, the transmitted signal should satisfy

$$\mathbb{E}[\|\mathbf{x}\|^2] = \sum_{i=1}^{M}\sum_{j\in\mathcal{G}_i}\mathbb{E}|x_j|^2 \le P. \tag{8}$$

Now, we consider the user k when served by the mth beam, i.e., $k \in \mathcal{G}_m$. Then, the received signal at the user k becomes

$$\begin{aligned} y_k &= \mathbf{h}_k^\dagger\left(\sum_{i=1}^{M}\sum_{j\in\mathcal{G}_i}\mathbf{v}_i x_j\right) + n_k\\ &= \mathbf{h}_k^\dagger\mathbf{v}_m x_k + \mathbf{h}_k^\dagger\mathbf{v}_m\Bigg(\sum_{i\in\mathcal{G}_m\setminus\{k\}} x_i\Bigg)\end{aligned}$$

[1]For a positive integer N, we denote by $[N]$ the set of all positive integers less than or equal to N, i.e., $[N] \triangleq \{1, \ldots, N\}$.

$$\mathbf{h}_k(t, f_c) = \left[\sqrt{\frac{\eta_k}{\eta_k+1}}\xi_k e^{j2\pi(f_k^{\text{D,LoS}} - f_c\tau_k^{\text{LoS}})} + \sqrt{\frac{1}{L_k(\eta_k+1)}}\sum_{l=1}^{L_k}\left[\xi_{k,l}e^{j2\pi(f_{k,l}^{\text{D,NLoS}} - f_c\tau_{k,l}^{\text{NLoS}})}\right]\right]\mathbf{u}_k(\theta_k^{\text{LoS}}, \psi_k^{\text{LoS}}). \tag{6}$$

$$+\mathbf{h}_k^{\dagger}\Bigg(\sum_{i\in[M]\setminus\{m\}}\sum_{j\in\mathcal{G}_i}\mathbf{v}_i x_j\Bigg)+n_k, \tag{9}$$

where $\setminus$ denotes set difference. In (9), the term $\mathbf{h}_k^{\dagger}\mathbf{v}_m x_k$ is the desired signal of the user k, while the terms $\mathbf{h}_k^{\dagger}\mathbf{v}_m\big(\sum_{i\in\mathcal{G}_m\setminus\{k\}}x_i\big)$ and $\mathbf{h}_k^{\dagger}\big(\sum_{i\in[M]\setminus\{m\}}\sum_{j\in\mathcal{G}_i}\mathbf{v}_i x_j\big)$ are the intra-beam interference and the inter-beam interference, respectively. In this case, the SINR of the user k becomes

$$\mathsf{SINR}_k=\frac{|\mathbf{h}_k^{\dagger}\mathbf{v}_m|^2P_k}{|\mathbf{h}_k^{\dagger}\mathbf{v}_m|^2\sum\limits_{i\in\mathcal{G}_m\setminus\{k\}}P_i+\sum\limits_{i\in[M]\setminus\{m\}}\sum\limits_{j\in\mathcal{G}_i}P_j|\mathbf{h}_k^{\dagger}\mathbf{v}_i|^2+1}, \tag{10}$$

and the corresponding achievable rate becomes $\log_2(1+\mathsf{SINR}_k)$.

In the next section, we propose our random-beam based NOMA, where the intra-beam interference is suppressed with NOMA (i.e., SIC among the users in the same user group), while the inter-beam interference is managed by random beamforming with user selection (i.e., user diversity).

Lemma 1 (Average Channel Gain): When the user k is served by the beam i (i.e., $\mathbf{v}_i$), the average channel gain is mainly determined by the direction of the LoS path as follows:

$$\mathbb{E}[|\mathbf{h}_k^{\dagger}\mathbf{v}_i|^2]=\mathbb{E}[\|\mathbf{h}_k\|^2]\cdot|\mathbf{u}_k(\theta_k^{\mathrm{LoS}},\psi_k^{\mathrm{LoS}})^{\dagger}\mathbf{v}_i|^2. \tag{11}$$

Proof: We can readily obtain (11) from (6), so omit the detailed proof. □

From now, we denote by Γ_k^i the average channel gain of the user k when served by the beam i (i.e., $\mathbf{v}_i$), which is given by

$$\Gamma_k^i\triangleq\mathbb{E}[|\mathbf{h}_k^{\dagger}\mathbf{v}_i|^2]=\mathbb{E}[\|\mathbf{h}_k\|^2]\cdot|\mathbf{u}_k(\theta_k^{\mathrm{LoS}},\psi_k^{\mathrm{LoS}})^{\dagger}\mathbf{v}_i|^2. \tag{12}$$

III. RANDOM BEAM-BASED NON-ORTHOGONAL MULTIPLE ACCESS

In this section, we propose random beam-based NOMA for massive MIMO LEO satellite communication systems. We first explain the procedure of our proposed scheme and find the achievable SINR with the instantaneous CSI. Then, we modify our proposed scheme for the use of the statistical CSI.

A. THE PROCEDURE OF OUR RANDOM BEAM-BASED NOMA AND THE ACHIEVABLE SINR WITH THE INSTANTANEOUS CSI

The procedure of our random beam-based NOMA is as follows:

- The satellite broadcasts M orthogonal random beams.
- Each user feeds several scalar values back to the satellite. (The feedback information will be discussed later.)
- With the collected feedback information, the satellite finds NOMA user groups $\mathcal{G}_1,\ldots,\mathcal{G}_M$ with power allocation, where $\mathcal{G}_m$ is the user group supported by the mth beam with NOMA.
- The satellite serves the user groups using the random beams with NOMA.

In our proposed scheme, the satellite uses M orthogonal random beams $\mathbf{v}_1,\ldots,\mathbf{v}_M\in\mathbb{C}^{N_xN_y\times 1}$ that are unit vectors and pairwise orthogonal to each other, i.e., $\|\mathbf{v}_1\|^2=\ldots=\|\mathbf{v}_M\|^2=1$ such that $\mathbf{v}_i\perp\mathbf{v}_j$ whenever $i\neq j$. Then, the mth beam supports the user group $\mathcal{G}_m$ with NOMA. For notational simplicity in the latter part of the paper, we denote by π_m the *reverse* decoding order for SIC among the users in the user group $\mathcal{G}_m$ as follows:

$$\pi_m\triangleq[\pi_m^{(1)},\ldots,\pi_m^{(|\mathcal{G}_m|)}], \tag{13}$$

where $|\cdot|$ represents the set cardinality. Thus, every user in $\mathcal{G}_m$ decodes the user $\pi_m^{(|\mathcal{G}_m|)}$'s data first and then subtracts it from the received signal. In this way, the user $\pi_m^{(l)}$ decodes and subtracts the signals of users $\pi_m^{(l+1)},\ldots,\pi_m^{|\mathcal{G}_m|}$. As a result, the user $\pi_m^{(|\mathcal{G}_m|)}$ decodes its own signal treating all other users' data as noises, while the user $\pi_m^{(1)}$ decodes its own signal without any interference (by subtracting all other users' data from its received signal).

Now, we consider the user $\pi_m^{(l)}$, who is the user at the $(|\mathcal{G}_m|-l+1)$th decoding order in the user group $\mathcal{G}_m$. Then, the received signal at the user $\pi_m^{(l)}$ becomes

$$\begin{aligned}y_{\pi_m^{(l)}}&=\mathbf{h}_{\pi_m^{(l)}}^{\dagger}\mathbf{v}_m x_{\pi_m^{(l)}}+\mathbf{h}_{\pi_m^{(l)}}^{\dagger}\mathbf{v}_m\Bigg(\sum_{i=1}^{l-1}x_{\pi_m^{(i)}}\Bigg)\\&+\mathbf{h}_{\pi_m^{(l)}}^{\dagger}\mathbf{v}_m\Bigg(\sum_{i=l+1}^{|\mathcal{G}_m|}x_{\pi_m^{(i)}}\Bigg)\\&+\mathbf{h}_{\pi_m^{(l)}}^{\dagger}\Bigg(\sum_{i\in[M]\setminus\{m\}}\sum_{j\in\mathcal{G}_i}\mathbf{v}_i x_j\Bigg)+n_{\pi_m^{(l)}}.\end{aligned} \tag{14}$$

When the SIC is perfect, the user $\pi_m^{(l)}$ can subtract the decoded signals of the users $\pi_m^{(l+1)},\ldots,\pi_m^{|\mathcal{G}_m|}$, and hence can subtract the term $\mathbf{h}_{\pi_m^{(l)}}^{\dagger}\mathbf{v}_m\big(\sum_{i=l+1}^{|\mathcal{G}_m|}x_{\pi_m^{(i)}}\big)$ from the received signal, so (14) becomes

$$\begin{aligned}y_{\pi_m^{(l)}}&=\mathbf{h}_{\pi_m^{(l)}}^{\dagger}\mathbf{v}_m x_{\pi_m^{(l)}}+\mathbf{h}_{\pi_m^{(l)}}^{\dagger}\mathbf{v}_m\Bigg(\sum_{i=1}^{l-1}x_{\pi_m^{(i)}}\Bigg)\\&+\mathbf{h}_{\pi_m^{(l)}}^{\dagger}\Bigg(\sum_{i\in[M]\setminus\{m\}}\sum_{j\in\mathcal{G}_i}\mathbf{v}_i x_j\Bigg)+n_{\pi_m^{(l)}}.\end{aligned} \tag{15}$$

In this case, the corresponding SINR becomes

$$\mathsf{SINR}^{\star}_{\pi_m^{(l)}}=\frac{|\mathbf{h}_{\pi_m^{(l)}}^{\dagger}\mathbf{v}_m|^2P_{\pi_m^{(l)}}}{\mathtt{I}^{\mathsf{intra}}_{\pi_m^{(l)}}+\mathtt{I}^{\mathsf{inter}}_{\pi_m^{(l)}}+1}, \tag{16}$$

where $\mathtt{I}^{\mathsf{intra}}_{\pi_m^{(l)}}$ is the intra-beam interference power, and $\mathtt{I}^{\mathsf{inter}}_{\pi_m^{(l)}}$ is the inter-beam interference power given respectively by

$$\begin{aligned}\mathtt{I}^{\mathsf{intra}}_{\pi_m^{(l)}}&\triangleq|\mathbf{h}_{\pi_m^{(l)}}^{\dagger}\mathbf{v}_m|^2\cdot\Bigg[\sum_{i=1}^{l-1}P_{\pi_m^{(i)}}\Bigg]\\\mathtt{I}^{\mathsf{inter}}_{\pi_m^{(l)}}&\triangleq\sum_{i\in[M]\setminus\{m\}}\sum_{j\in\mathcal{G}_i}\Bigg[P_j|\mathbf{h}_{\pi_m^{(l)}}^{\dagger}\mathbf{v}_i|^2\Bigg].\end{aligned} \tag{17}$$

In our proposed scheme, we consider the equal power allocation over the beams given by

$$\sum_{i\in\mathcal{G}_m} P_i \leq \frac{P}{M} \text{ for all } m \in [M]. \tag{18}$$

Allocating more power to a beam can increase the inter-beam interference at other beams, which makes our problem more complex. Thus, with the equal power allocation over the beams, we can reduce the computational complexity for beam power allocation. Under this setting, the inter-beam interference power in (17) can be upper bounded as follows:

$$\begin{aligned}\mathrm{I}^{\text{inter}}_{\pi_m^{(l)}} &\triangleq \sum_{i\in[M]\setminus\{m\}} \sum_{j\in\mathcal{G}_i} P_j |\mathbf{h}^\dagger_{\pi_m^{(l)}} \mathbf{v}_i|^2 \\ &= \sum_{i\in[M]\setminus\{m\}} \left[|\mathbf{h}^\dagger_{\pi_m^{(l)}} \mathbf{v}_i|^2 \left(\sum_{j\in\mathcal{G}_i} P_j \right) \right] \\ &\overset{(a)}{\leq} \frac{P}{M} \cdot \sum_{i\in[M]\setminus\{m\}} |\mathbf{h}^\dagger_{\pi_m^{(l)}} \mathbf{v}_i|^2, \end{aligned} \tag{19}$$

where the inequality (a) is from (18).

Now, we consider NOMA at each beam. In the NOMA user group $\mathcal{G}_m$ at the mth beam, for all users' successful decodings with the reverse decoding order π_m, all users' SINR values should satisfy that

$$\mathsf{SINR}^\star_{\pi_m^{(l)}} \geq \gamma \quad \text{for all } \ l \in \pi_m. \tag{20}$$

In practice, however, the perfect SIC is almost impossible especially in satellite communications because the perfect CSI at the satellite is very hard. In this case, one way to model the imperfectness of SIC is to consider the imperfect SIC parameter [20]; with the imperfect SIC parameter $\mu \in [0, 1]$, the SINR of the user $\pi_m^{(l)}$ becomes

$$\mathsf{SINR}_{\pi_m^{(l)}} \triangleq \frac{|\mathbf{h}^\dagger_{\pi_m^{(l)}} \mathbf{v}_m|^2 P_{\pi_m^{(l)}}}{\mathrm{I}^{\text{intra}}_{\pi_m^{(l)}} + \mathrm{I}^{\text{SIC}}_{\pi_m^{(l)}} + \mathrm{I}^{\text{inter}}_{\pi_m^{(l)}} + 1}, \tag{21}$$

where $\mathrm{I}^{\text{SIC}}_{\pi_m^{(l)}}$ is the residual interference power due to the imperfect SIC given by

$$\mathrm{I}^{\text{SIC}}_{\pi_m^{(l)}} \triangleq |\mathbf{h}^\dagger_{\pi_m^{(l)}} \mathbf{v}_m|^2 \cdot \left(\sum_{i=l+1}^{|\mathcal{G}_m|} \mu P_{\pi_m^{(i)}} \right). \tag{22}$$

Thus, our original problem (with instantaneous CSI) becomes to find user selection (i.e., NOMA user groups $\mathcal{G}_1, \ldots, \mathcal{G}_M$) and power allocation $\{P^{(1)}_{\pi_m}, \ldots, P^{(|\mathcal{G}_m|)}_{\pi_m}\}_{m=1}^M$ as follows:

$$\begin{aligned} \textbf{(P0)} \ \underset{\substack{\mathcal{G}_1,\ldots,\mathcal{G}_M \subset [K], \\ \{P^{(1)}_{\pi_m},\ldots,P^{(|\mathcal{G}_m|)}_{\pi_m}\}_{m=1}^M}}{\text{maximize}} \ & \sum_{m=1}^{M} \sum_{l=1}^{|\mathcal{G}_m|} \mathbf{1}(\mathsf{SINR}_{\pi_m^{(l)}} \geq \gamma) \\ \text{subject to} \quad & \mathcal{G}_i \cap \mathcal{G}_j = \phi \ \text{ for all } \ i \neq j, \qquad (23) \\ & \sum_{i\in\mathcal{G}_m} P_i \leq \frac{P}{M} \ \text{ for all } \ m \in [M]. \qquad (24) \end{aligned}$$

B. THE RANDOM BEAM-BASED NOMA WITH THE STATISTICAL CSI

In this subsection, we explain our proposed scheme operated with statistical CSI. In satellite communications, even the perfect instantaneous CSI cannot be directly exploited at the satellite because of the propagation delay. This is because the instantaneous CSI at the satellite has already been outdated when the user receives the signal. Thus, it makes more sense to consider the statistical CSI for beamforming.

In the next subsections, we first find the average SINR at the selected user and its bounds. Then, we propose two random beam-based NOMA schemes with different complexities and feedback overheads.

1) AVERAGE SINR AT THE SELECTED USER

From (21), we define the average SINR of the user $\pi_m^{(l)}$ as follows:

$$\mathsf{ASINR}_{\pi_m^{(l)}} \triangleq \frac{\mathbb{E}\left\{ |\mathbf{h}^\dagger_{\pi_m^{(l)}} \mathbf{v}_m|^2 P_{\pi_m^{(l)}} \right\}}{\mathbb{E}\left\{\mathrm{I}^{\text{intra}}_{\pi_m^{(l)}}\right\} + \mathbb{E}\left\{\mathrm{I}^{\text{SIC}}_{\pi_m^{(l)}}\right\} + \mathbb{E}\left\{\mathrm{I}^{\text{inter}}_{\pi_m^{(l)}}\right\} + 1}. \tag{25}$$

Using the notation defined in (12), we can find that

$$\begin{aligned} \mathbb{E}\left\{ |\mathbf{h}^\dagger_{\pi_m^{(l)}} \mathbf{v}_m|^2 P_{\pi_m^{(l)}} \right\} &= \mathbb{E}\left\{ |\mathbf{h}^\dagger_{\pi_m^{(l)}} \mathbf{v}_m|^2 \right\} \cdot P_{\pi_m^{(l)}} \\ &= \Gamma^m_{\pi_m^{(l)}} \cdot P_{\pi_m^{(l)}}. \end{aligned} \tag{26}$$

Similarly, we have

$$\begin{aligned} \mathbb{E}\left\{\mathrm{I}^{\text{intra}}_{\pi_m^{(l)}}\right\} &= \mathbb{E}\left\{ |\mathbf{h}^\dagger_{\pi_m^{(l)}} \mathbf{v}_m|^2 \cdot \left(\sum_{i=1}^{l-1} P_{\pi_m^{(i)}} \right) \right\} \\ &= \Gamma^m_{\pi_m^{(l)}} \cdot \left(\sum_{i=1}^{l-1} P_{\pi_m^{(i)}} \right) \end{aligned} \tag{27}$$

$$\begin{aligned} \mathbb{E}\left\{\mathrm{I}^{\text{SIC}}_{\pi_m^{(l)}}\right\} &= \mathbb{E}\left\{ |\mathbf{h}^\dagger_{\pi_m^{(l)}} \mathbf{v}_m|^2 \cdot \left(\sum_{i=l+1}^{|\mathcal{G}_m|} \mu P_{\pi_m^{(i)}} \right) \right\} \\ &= \Gamma^m_{\pi_m^{(l)}} \cdot \left(\sum_{i=l+1}^{|\mathcal{G}_m|} \mu P_{\pi_m^{(i)}} \right) \end{aligned} \tag{28}$$

$$\begin{aligned} \mathbb{E}\left\{\mathrm{I}^{\text{inter}}_{\pi_m^{(l)}}\right\} &= \mathbb{E}\left\{ \sum_{i\in[M]\setminus\{m\}} \sum_{j\in\mathcal{G}_i} P_j |\mathbf{h}^\dagger_{\pi_m^{(l)}} \mathbf{v}_i|^2 \right\} \\ &= \sum_{i\in[M]\setminus\{m\}} \sum_{j\in\mathcal{G}_i} P_j \cdot \Gamma^i_{\pi_m^{(l)}} \\ &= \sum_{i\in[M]\setminus\{m\}} \left[\Gamma^i_{\pi_m^{(l)}} \cdot \left(\sum_{j\in\mathcal{G}_i} P_j \right) \right]. \end{aligned} \tag{29}$$

Then, plugging (26)-(29) into (25), we obtain (30), as shown at the bottom of the next page.

We also modify the QoS constraint in the average sense, so the QoS constraint given in (20) is relaxed to

$$\mathsf{ASINR}_{\pi_m^{(l)}} \geq \gamma \quad \text{for all } \ l \in \pi_m. \tag{31}$$

Thus, with the statistical CSI, the problem **(P0)** is changed to the problem **(P1)** as follows:

$$\textbf{(P1)} \quad \underset{\substack{\mathcal{G}_1,\ldots,\mathcal{G}_M \subset [K], \\ \{P^{(1)}_{\pi_m},\ldots,P^{(|\mathcal{G}_m|)}_{\pi_m}\}_{m=1}^{M}}}{\text{maximize}} \sum_{m=1}^{M}\sum_{l=1}^{|\mathcal{G}_m|} \mathbf{1}(\mathsf{ASINR}_{\pi_m^{(l)}} \geq \gamma)$$
$$\text{subject to} \quad (23), (24).$$

However, the problem **(P1)** is hard to solve. In general, a user selection (or grouping) problem can be regarded as allocating zero or one to each user, so is a mixed integer problem generally known as an NP-hard problem. Moreover, as we can see in (30), the SINR of a user is affected by not only power allocations at other beams but also power allocation for NOMA at the same beam. Thus, we need to modify the problem **(P1)** for tractability.

In the denominator of (25), we have

$$\begin{aligned} &\mathbb{E}\left\{\mathrm{I}^{\text{intra}}_{\pi_m^{(l)}}\right\} + \mathbb{E}\left\{\mathrm{I}^{\text{SIC}}_{\pi_m^{(l)}}\right\} \\ &= \Gamma^m_{\pi_m^{(l)}}\left[\sum_{i=1}^{l-1} P_{\pi_m^{(i)}} + \sum_{i=l+1}^{|\mathcal{G}_m|} \mu P_{\pi_m^{(i)}}\right] \\ &\overset{(a)}{\leq} \Gamma^m_{\pi_m^{(l)}}\left[(1-\mu)\sum_{i=1}^{l-1} P_{\pi_m^{(i)}} + \mu\frac{P}{M} - \mu P_{\pi_m^{(l)}}\right], \end{aligned} \tag{32}$$

where the inequality (a) holds because

$$\sum_{i=l+1}^{|\mathcal{G}_m|} \mu P_{\pi_m^{(i)}} \leq \mu\left(\frac{P}{M} - \sum_{i=1}^{l-1} P_{\pi_m^{(i)}} - P_{\pi_m^{(l)}}\right). \tag{33}$$

Thus, plugging the right-hand side of (32) into (30), we obtain (34), as shown at the bottom of the page, which is the lower bound of $\mathsf{ASINR}_{\pi_m^{(l)}}$ such that

$$\overline{\mathsf{ASINR}}_{\pi_m^{(l)}} \leq \mathsf{ASINR}_{\pi_m^{(l)}}. \tag{35}$$

Meanwhile, the average inter-beam interference $\mathbb{E}\{\mathrm{I}^{\text{inter}}_{\pi_m^{(l)}}\}$ in (29) is upper bounded as

$$\mathbb{E}\left\{\mathrm{I}^{\text{inter}}_{\pi_m^{(l)}}\right\} \overset{(a)}{\leq} \frac{P}{M}\sum_{i\in[M]\setminus\{m\}} \Gamma^i_{\pi_m^{(l)}}, \tag{36}$$

where the inequality (a) is from the constraint (18). Thus, applying the bound (36) into (34), we obtain the further lowerer bound $\overline{\mathsf{ASINR}}^{\downarrow}_{\pi_m^{(l)}}$ such that

$$\overline{\mathsf{ASINR}}^{\downarrow}_{\pi_m^{(l)}} \leq \overline{\mathsf{ASINR}}_{\pi_m^{(l)}}, \tag{37}$$

which is given by

$$\overline{\mathsf{ASINR}}^{\downarrow}_{\pi_m^{(l)}} = \frac{\Gamma^m_{\pi_m^{(l)}} \cdot P_{\pi_m^{(l)}}}{\Gamma^m_{\pi_m^{(l)}}\left[\sum_{i=1}^{l-1} P_{\pi_m^{(i)}} + \sum_{i=l+1}^{|\mathcal{G}_m|} \mu P_{\pi_m^{(i)}}\right] + \frac{P}{M}\sum_{i\in[M]\setminus\{m\}} \Gamma^i_{\pi_m^{(l)}} + 1}. \tag{38}$$

Thus, from the relationships (35) and (37), we have

$$\mathsf{ASINR}_{\pi_m^{(l)}} \geq \overline{\mathsf{ASINR}}_{\pi_m^{(l)}} \geq \overline{\mathsf{ASINR}}^{\downarrow}_{\pi_m^{(l)}}. \tag{39}$$

Thus, the average QoS constraint at the mth beam

$$\overline{\mathsf{ASINR}}_{\pi_m^{(l)}} \geq \gamma \quad \text{for all } l \in \pi_m \tag{40}$$

is tighter than (31), and the constraint

$$\overline{\mathsf{ASINR}}^{\downarrow}_{\pi_m^{(l)}} \geq \gamma \quad \text{for all } l \in \pi_m \tag{41}$$

is even more tight.

In next subsections, we propose two random-beam based NOMA schemes replacing the average QoS constraint (31) into two more tight constraints (40) and (41), respectively.

2) PROPOSED SCHEME 1

In our first proposed scheme, we consider the constraint (40) at each beam. In this case, the problem **(P1)** is changed to the problem **(P2)** as follows:

$$\textbf{(P2)} \quad \underset{\substack{\mathcal{G}_1,\ldots,\mathcal{G}_M \subset [K], \\ \{P^{(1)}_{\pi_m},\ldots,P^{(|\mathcal{G}_m|)}_{\pi_m}\}_{m=1}^{M}}}{\text{maximize}} \sum_{m=1}^{M}\sum_{l=1}^{|\mathcal{G}_m|} \mathbf{1}(\overline{\mathsf{ASINR}}_{\pi_m^{(l)}} \geq \gamma)$$
$$\text{subject to} \quad (23), (24).$$

and our first proposed scheme solves the problem **(P2)**.

$$\mathsf{ASINR}_{\pi_m^{(l)}} = \frac{\Gamma^m_{\pi_m^{(l)}} \cdot P_{\pi_m^{(l)}}}{\Gamma^m_{\pi_m^{(l)}}\left[\sum_{i=1}^{l-1} P_{\pi_m^{(i)}} + \sum_{i=l+1}^{|\mathcal{G}_m|} \mu P_{\pi_m^{(i)}}\right] + \sum_{i\in[M]\setminus\{m\}}\left[\Gamma^i_{\pi_m^{(l)}} \cdot \left(\sum_{j\in\mathcal{G}_i} P_j\right)\right] + 1}. \tag{30}$$

$$\overline{\mathsf{ASINR}}_{\pi_m^{(l)}} = \frac{\Gamma^m_{\pi_m^{(l)}} \cdot P_{\pi_m^{(l)}}}{\Gamma^m_{\pi_m^{(l)}}\left[(1-\mu)\sum_{i=1}^{l-1} P_{\pi_m^{(i)}} + \mu\frac{P}{M} - \mu P_{\pi_m^{(l)}}\right] + \sum_{i\in[M]\setminus\{m\}}\left[\Gamma^i_{\pi_m^{(l)}} \cdot \left(\sum_{j\in\mathcal{G}_i} P_j\right)\right] + 1}. \tag{34}$$

For given power allocation, to calculate the user $\pi_m^{(l)}$'s average SINR bound given in (34), the satellite requires the following M scalar values

$$\Gamma^1_{\pi_m^{(l)}}, \ldots, \Gamma^M_{\pi_m^{(l)}}. \tag{42}$$

Thus, in our first proposed scheme, each user feeds M scalar values to aid the satellite's user selection and power allocation; the user k feeds the following information back to the satellite:

$$\left\{\Gamma^1_k, \ldots, \Gamma^M_k\right\}, \tag{43}$$

where the M scalar values correspond to the *average* channel gains from M beams, respectively.

3) PROPOSED SCHEME 2

In our second proposed scheme, we consider the constraint (41) at each beam. In this case, the problem **(P1)** is changed to the problem **(P3)** as follows:

$$\textbf{(P3)} \quad \underset{\substack{\mathcal{G}_1,\ldots,\mathcal{G}_M\subset[K],\\ \{P^{(1)}_{\pi_m},\ldots,P^{(|\mathcal{G}_m|)}_{\pi_m}\}_{m=1}^M}}{\text{maximize}} \sum_{m=1}^{M}\sum_{l=1}^{|\mathcal{G}_m|} \mathbf{1}(\overline{\mathsf{ASINR}}^{\downarrow}_{\pi_m^{(l)}} \geq \gamma)$$
$$\text{subject to} \quad (23), (24).$$

and our second proposed scheme solves the problem **(P3)**.

Note that for given power allocation, to calculate the user $\pi_m^{(l)}$'s average SINR bound given in (38), the satellite needs to obtain the following two scalar values

$$\Gamma^m_{\pi_m^{(l)}}, \sum_{i\in[M]\backslash\{m\}} \Gamma^i_{\pi_m^{(l)}} \tag{44}$$

from the user $\pi_m^{(l)}$.

Thus, in our second proposed scheme, each user feeds three values[2] to aid the satellite's user selection and power allocation; the user k feeds the following information back to the satellite:

$$\left\{\mathcal{I}(k),\ \Gamma^{\mathcal{I}(k)}_k,\ \sum_{i\in[M]\backslash\{\mathcal{I}(k)\}} \Gamma^i_k\right\}, \tag{45}$$

where $\mathcal{I}(\cdot)$ is the selected beam indicator given by

$$\mathcal{I}(k) = \arg\max_{m\in[M]} \Gamma^m_k. \tag{46}$$

Note that these three feedback values correspond to 1) the selected beam index with the *averaged* channel, 2) the *average* channel gain with the selected beam, 3) the sum of *average* channel gains with the other beams, respectively.

Remark 1: Note that in the both of our proposed schemes, each user's feedback information is based on the statistical CSI. In the first scheme, each user feeds M scalar values, while in the second scheme, each user feeds two scalar values with $\log_2 M$ bits. Thus, the feedback overheads are relatively very small compared to the statistical channel vector feedback, which is comprised of $2N_xN_y$ scalar values to represent an N_xN_y-dimensional complex vector.

[2] When $M = 2$, we only need two scalar value feedback $\{\Gamma^1_k, \Gamma^2_k\}$ for user k because $\mathcal{I}(k) = \arg\max_{i\in[2]} \Gamma^i_k$.

IV. OPTIMIZATION OF OUR PROPOSED RANDOM BEAM-BASED NOMA

As we mentioned earlier, our first proposed scheme solves the problem **(P2)**, and the second proposed scheme solves the problem **(P3)**. In this section, we solve the problem **(P2)** and the problem **(P3)**, respectively.

A. THE SOLUTION OF THE problem (P2)

In this subsection, we solve the problem **(P2)**. We recall the problem **(P2)** as follows:

$$\textbf{(P2)} \quad \underset{\substack{\mathcal{G}_1,\ldots,\mathcal{G}_M\subset[K],\\ \{P^{(1)}_{\pi_m},\ldots,P^{(|\mathcal{G}_m|)}_{\pi_m}\}_{m=1}^M}}{\text{maximize}} \sum_{m=1}^{M}\sum_{l=1}^{|\mathcal{G}_m|} \mathbf{1}(\overline{\mathsf{ASINR}}_{\pi_m^{(l)}} \geq \gamma)$$
$$\text{subject to} \quad (23), (24).$$

As we can see in (34), the user selection and the power allocation at a beam is affected by the other beams' user selections and power allocations. Thus, the problem **(P2)** is still NP-hard, and the optimal solution is not easy to find.

As a suboptimal solution, we propose an iterative way to solve problem **(P2)**; the main idea is to iteratively update user groups and power allocations considering the *fixed* inter-beam interference found at the previous iteration. From the constraint (40), we can find the power allocation to the user of the $(|\mathcal{G}_m| - l + 1)$th decoding order (i.e., the user $\pi_m^{(l)}$) in (47), as shown at the bottom of the next page.

Then, for iterative calculation, we rewrite (47) into (48), as shown at the bottom of the next page, where the superscript $(\cdot)^{\langle n\rangle}$ denotes the result at the nth iteration. Then, we obtain the following Remark.

Remark 2: In (48), we can observe that the user selection at the beam m is invariant with the user selection at the other beams. This is because at each iteration, we assume the fixed inter-beam interference (e.g., in (48),

$$\sum_{i\in[M]\backslash\{m\}} \left[\Gamma^i_{\pi_m^{(l)}} \cdot \left(\sum_{j\in\mathcal{G}_i^{\langle n-1\rangle}} P_j^{\langle n-1\rangle}\right)\right]$$

at the user $\pi_m^{(l)}$), which is mainly determined by the correlations of a user's channel to the other beam directions. This fact gives us an important intuition that at each iteration, we need to solve M independent sub-problems, each of which corresponds to user selection and power allocation at each beam.

With the initial setting

$$\mathcal{G}_m^{\langle 0\rangle} = \left\{k \in [K] \;\middle|\; \max_{i\in[M]} \Gamma^i_k = \Gamma^m_k\right\} \tag{49}$$

and $P_1^{\langle 0\rangle} = \ldots = P_K^{\langle 0\rangle} = 0$, in the first iteration, each beam finds the NOMA user group and power allocation with the power budget. Then, at the iteration n, each beam finds the largest NOMA user group $\mathcal{G}_m^{\langle n\rangle}$ such that $\mathcal{G}_m^{\langle n\rangle} \subset \mathcal{G}_m^{\langle n-1\rangle}$ for all $m \in [M]$ considering the inter-beam interference calculated at the $(n-1)$th iteration. This is because the iteration starts from the zero inter-beam interference setting, and this setting ensures the convergence of the solution.

Regarding user grouping and power allocation, we can observe from (48) that the power allocation $P^{\langle n\rangle}_{\pi_m^{(l)}}$ is only dependent on the values of $P^{\langle n\rangle}_{\pi_m^{(1)}}, \ldots, P^{\langle n\rangle}_{\pi_m^{(l-1)}}$. Thus, once an arbitrary NOMA user group is given, we can check whether each beam can support the arbitrary NOMA user group with the power budget; we first find the required power for the user of the last decoding order, i.e., $P^{\langle n\rangle}_{\pi_m^{(1)}}$, and then sequentially find the required powers of the other users according to the reverse decoding order, i.e., $P_{\pi_m^{(2)}}, \ldots, P_{\pi_m^{(|\mathcal{G}_m|)}}$ in sequence. Then, we can know whether the arbitrary NOMA group is feasible by checking the beam power constraint (50) holds. In this way, each beam can find the largest NOMA user group and the power allocation at each iteration. We summarize the procedure to solve the problem (P2) in Algorithm 1.

B. THE SOLUTION OF THE problem (P3)

In this subsection, we solve the problem (P3). We recall the problem (P3) as follows:

$$\text{(P3)} \quad \underset{\substack{\mathcal{G}_1,\ldots,\mathcal{G}_M \subset [K],\\ \{P^{(1)}_{\pi_m},\ldots,P^{(|\mathcal{G}_m|)}_{\pi_m}\}_{m=1}^M}}{\text{maximize}} \sum_{m=1}^{M}\sum_{l=1}^{|\mathcal{G}_m|} \mathbf{1}(\overline{\mathsf{ASINR}}^{\downarrow}_{\pi_m^{(l)}} \geq \gamma)$$
$$\text{subject to} \qquad (23), (24).$$

Then, we start from the following remark.

Remark 3: Similarly with **Remark 2**, *we can observe in (38) that the user selection at the beam m is invariant with the user selection at the other beams. This is because we assume the maximum (fixed) inter-beam interference (e.g., in (38), $\frac{P}{M}\sum_{i\in[M]\setminus\{m\}}\Gamma^i_{\pi_m^{(l)}}$ for user $\pi_m^{(i)}$), which is mainly determined by the correlations of a user's channel to the other beam directions. Thus, the problem (P3) can also be divided into M independent sub-problems, where each sub-problem corresponds to user selection and power allocation at each beam.*

Thus, for the mth beam, the satellite solves the following problem:

$$\text{(P4)} \quad \underset{\mathcal{G}_m, P^{(1)}_{\pi_m},\cdots,P^{(|\mathcal{G}_m|)}_{\pi_m}}{\text{maximize}} \sum_{l=1}^{|\mathcal{G}_m|} \mathbf{1}(\overline{\mathsf{ASINR}}^{\downarrow}_{\pi_m^{(l)}} \geq \gamma)$$

Algorithm 1 The Procedure to Solve the problem **(P2)**

```
Result: The NOMA user groups G*_1, ..., G*_M and the
        power allocation {P^(1)_{π_m}, ..., P^(|G*_m|)_{π_m}}_{m=1}^M
Initial setup:
  Set NOMA user groups G^⟨0⟩_1, ..., G^⟨0⟩_M from (49)
  Set power allocation P^⟨0⟩_1 = ... = P^⟨0⟩_K = 0
  Set an iteration index n = 0
repeat
   n = n + 1
   for m = 1 to M do
      G^⟨n⟩_m = ∅ for i = 1 to |G^⟨n−1⟩_m| do
         P' = P'' = 0 for all G_m ⊂ G^⟨n−1⟩_m such
          that |G_m| = i do
            Find P^⟨n⟩_{π_m^(1)}, ..., P^⟨n⟩_{π_m^(|G_m|)} from (48)
            if the beam power constraint (24) is
             satisfied then
               P' = P^⟨n⟩_{π_m^(1)} + ··· + P^⟨n⟩_{π_m^(|G_m|)} if
                P'' = 0 then
                  G^⟨n⟩_m = G_m, P'' = P'
               else if P' < P'' then
                  G^⟨n⟩_m = G_m, P'' = P'
            end
         end
      end
   end
until user grouping and power allocation converge;
```

$$\text{subject to} \qquad \sum_{i\in\mathcal{G}_m} P_i \leq \frac{P}{M}. \tag{50}$$

Then, from the condition (41), we can find the power allocation to the user of the $(|\mathcal{G}_m| - l + 1)$th decoding order (i.e., the user $\pi_m^{(l)}$) as follows:

$$P_{\pi_m^{(l)}} = \frac{\Gamma^m_{\pi_m^{(l)}}\left[(1-\mu)\sum_{i=1}^{l-1}P_{\pi_m^{(i)}} + \mu\frac{P}{M}\right] + \frac{P}{M}\sum_{i\in[M]\setminus\{m\}}\Gamma^i_{\pi_m^{(l)}} + 1}{\Gamma^m_{\pi_m^{(l)}}(1/\gamma + \mu)}$$

$$P_{\pi_m^{(l)}} = \frac{\Gamma^m_{\pi_m^{(l)}}\left[(1-\mu)\sum_{i=1}^{l-1}P_{\pi_m^{(i)}} + \mu\frac{P}{M}\right] + \sum_{i\in[M]\setminus\{m\}}\left[\Gamma^i_{\pi_m^{(l)}}\cdot\left(\sum_{j\in\mathcal{G}_i}P_j\right)\right] + 1}{\Gamma^m_{\pi_m^{(l)}}(1/\gamma + \mu)}. \tag{47}$$

$$P^{\langle n\rangle}_{\pi_m^{(l)}} = \frac{\Gamma^m_{\pi_m^{(l)}}\left[(1-\mu)\sum_{i=1}^{l-1}P^{\langle n\rangle}_{\pi_m^{(i)}} + \mu\frac{P}{M}\right] + \sum_{i\in[M]\setminus\{m\}}\left[\Gamma^i_{\pi_m^{(l)}}\cdot\left(\sum_{j\in\mathcal{G}_i^{\langle n-1\rangle}}P_j^{\langle n-1\rangle}\right)\right] + 1}{\Gamma^m_{\pi_m^{(l)}}(1/\gamma + \mu)}. \tag{48}$$

Algorithm 2 The Procedure to Solve the problem **(P3)**

Result: The NOMA user groups $\mathcal{G}_1^*, \ldots, \mathcal{G}_M^*$ and the power allocation $\{P_{\pi_m}^{(1)}, \ldots, P_{\pi_m}^{(|\mathcal{G}_m^*|)}\}_{m=1}^{M}$

Initial setup:

Set NOMA user groups $\mathcal{G}_1', \ldots, \mathcal{G}_M'$ from (53)

for $m = 1$ *to* M **do**
- $\mathcal{G}_m^* = \emptyset$
- **for** $i = 1$ *to* $|\mathcal{G}_m'|$ **do**
  - **for** *all* $\mathcal{G}_m \subset \mathcal{G}_m'$ *such that* $|\mathcal{G}_m| = i$ **do**
    - Find $P_{\pi_m^{(1)}}, \ldots, P_{\pi_m^{(|\mathcal{G}_m|)}}$ from (51)
    - **if** *the sum power constraint (50) is satisfied* **then**
      - $\mathcal{G}_m^* = \mathcal{G}_m$
    - **end**
  - **end**
- **end**

end

$$= \frac{(1-\mu)\sum_{i=1}^{l-1} P_{\pi_m^{(i)}} + \mu\frac{P}{M}}{(1/\gamma+\mu)} + \frac{\frac{P}{M}\sum_{i\in[M]\setminus\{m\}} \Gamma_{\pi_m^{(l)}}^{i} + 1}{\Gamma_{\pi_m^{(l)}}^{m}(1/\gamma+\mu)}. \quad (51)$$

As we can see in (51), the power allocation $P_{\pi_m^{(l)}}$ is dependent on the values of $P_{\pi_m^{(1)}}, \ldots, P_{\pi_m^{(l-1)}}$. Thus, we first find the required power for the user of the last decoding order, i.e., $P_{\pi_m^{(1)}}$, where

$$P_{\pi_m^{(1)}} = \frac{\frac{P}{M}\left[\mu\Gamma_{\pi_m^{(l)}}^{m} + \sum_{i\in[M]\setminus\{m\}} \Gamma_{\pi_m^{(l)}}^{i}\right] + 1}{\Gamma_{\pi_m^{(l)}}^{m}(1/\gamma+\mu)}, \quad (52)$$

and then sequentially find the required powers of the other users according to the reverse decoding order, i.e., $P_{\pi_m^{(2)}}, \ldots, P_{\pi_m^{(|\mathcal{G}_m|)}}$ in sequence. In this case, the beam power constraint (50) should hold. Thus, once the user group $\mathcal{G}_m$ is given, we can check whether NOMA is possible among the users in the user group with the given power budget.

As a result, to solve the problem (P4), the satellite first finds the user group $\mathcal{G}_m'$ from the collected feedback information as follows:

$$\mathcal{G}_m' = \left\{k \in [K] \,\middle|\, \mathcal{I}(k) = m\right\}. \quad (53)$$

Then, the satellite finds the largest user group $\mathcal{G}_m^* \subset \mathcal{G}_m'$ that satisfies the total power constraint. We summarize this procedure in Algorithm 2.

V. NUMERICAL RESULTS

In this section, we evaluate our proposed scheme. For simulation environment, we assume that the horizontal angle and the vertical angle of each user's LoS path (θ_k^{LoS} and ψ_k^{LoS} for the user k) are uniformly distributed in the range of $[-1, 1]$, respectively. Meanwhile, the Rician factors in all users' channels are assumed to be identical to $\eta = 9$. Also, we assume that the number of NLoS paths is five for every user (i.e., $L_1 = \ldots = L_K = 5$), and the delays (e.g., τ_k^{LoS} and $\tau_{k,l}^{\text{NLoS}}$) can be perfectly compensated [23]. In all simulations, the target QoS is fixed to $\gamma = 1$.

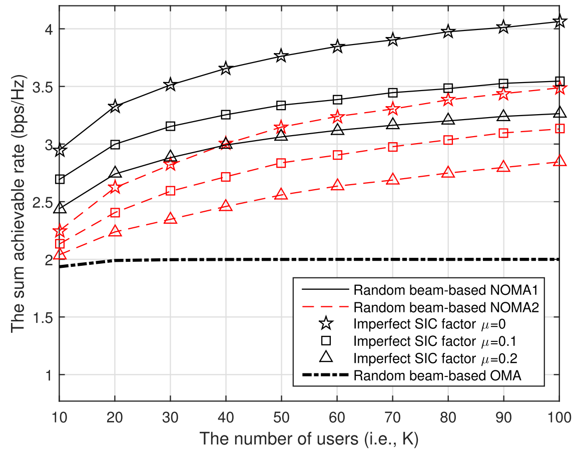

FIGURE 2. The achievable rate with respect to the number of users when the transmit SNR is fixed to 15 dB. The number of random beams is two (i.e., $M = 2$), and $N_x = N_y = 8$.

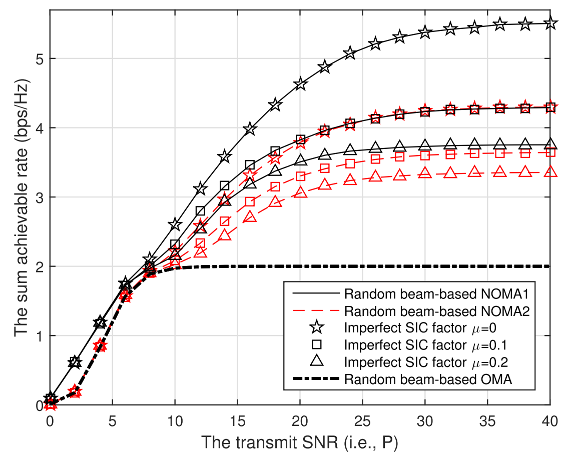

FIGURE 3. The achievable rate with respect to the transmit SNR when the number of users is fixed to 50. The number of random beams is two (i.e., $M = 2$), and $N_x = N_y = 8$.

As a reference scheme, we consider the conventional random beam based-OMA (i.e., random beamforming) with the average QoS constraint, where each user feeds the selected beam index with average SINR, i.e., for the user k,

$$\left\{\mathcal{I}(k),\ \frac{\frac{P}{M}\Gamma_k^{\mathcal{I}(k)}}{\frac{P}{M}\sum_{i\in[M]\setminus\{\mathcal{I}(k)\}} \Gamma_k^{i} + 1}\right\}, \quad (54)$$

so the feedback overhead from each user is $\log_2 M$ bits with a single scalar value. From the feedback value, each beam selects and serves a single user with the average QoS constraint.

In Fig. 2, we first show the achievable sum rate with respect to the number of users for various imperfect SIC factors (i.e., μ), where 'Random beam-based NOMA1' and 'Random beam-based NOMA2' correspond to our proposed schemes in Section III-B-II and Section III-B-III, respectively. We consider total 64 antennas at the satellite with the antenna configuration of $N_x = N_y = 8$, and the transmit SNR (i.e., P) is fixed to 15 dB. Also, we assume that the total number of random beams is two (i.e., $M = 2$). In Fig. 2, we can observe that the imperfectness of SIC reduces the achievable sum rates of our proposed random beam-based NOMA schemes. However, the achievable sum rates of our proposed schemes increase as the number of users increases regardless of the imperfect SIC factors, while the achievable sum rate of the random beam-based OMA is saturated as the number of users increases. This is because in our proposed schemes, each beam is more likely to support more than a single user as the number of users increases by enjoying more multiuser diversity. For each imperfect SIC factor, our first proposed scheme outperforms our second proposed scheme, and this is quite natural because the first proposed scheme takes more feedback information from each user and requires more computational complexity for power allocation.

In Fig. 3, we show the achievable sum rate with respect to the transmit SNR (i.e., P) for various imperfect SIC factors under the same antenna configuration when the number of users is fixed to 50 (i.e., $K = 50$). In this case, we also assume that the total number of random beams is two (i.e., $M = 2$). As we can see in Fig. 3, the achievable sum rates of our proposed schemes increase as the transmit SNR increases, while the random beam-based OMA is saturated at a high SNR region. This is because the conventional random beam-based OMA cannot support more than a single user at each beam, so cannot exploit the residual power once each beam fulfills a single user's QoS constraint. On the other hand, in our proposed schemes, the imperfectness of SIC reduces the achievable sum rate, but regardless of the imperfect SIC factors, the achievable sum rate increases as the transmit power increases. This is because in our proposed scheme, each beam is likely to support more users with NOMA with increased power. For each imperfect SIC factor, our first proposed scheme outperforms our second proposed scheme with the same reason in Fig. 2. In low SNR region, our first scheme far increases the performances of other two schemes, and this is because our first scheme considers more precise inter-beam interference, so streaming control is possible.

VI. CONCLUSION

In this paper, we proposed random beam-based NOMA for FDD massive MIMO LEO satellite communication systems. In our random beam-based NOMA, the satellite exploits random beams, where each beam can support multiple users with NOMA. Meanwhile, to aid the satellite's user selection and power allocation, each user feeds several scalar values back to the satellite, which is obtained from statistical CSI. We proposed two random beam-based NOMA schemes of different complexities and feedback overheads and optimized our proposed schemes by solving joint user selection and power allocation problems. The numerical result showed that our proposed schemes outperform the conventional random beamforming, i.e., OMA at each beam, by supporting more users at each beam.

REFERENCES

[1] A. Guidotti, A. Vanelli-Coralli, M. Conti, S. Andrenacci, S. Chatzinotas, N. Maturo, B. Evans, A. Awoseyila, A. Ugolini, T. Foggi, L. Gaudio, N. Alagha, and S. Cioni, "Architectures and key technical challenges for 5G systems incorporating satellites," *IEEE Trans. Veh. Technol.*, vol. 68, no. 3, pp. 2624–2639, Mar. 2019.

[2] B. Di, L. Song, Y. Li, and H. V. Poor, "Ultra-dense LEO: Integration of satellite access networks into 5G and beyond," *IEEE Wireless Commun.*, vol. 26, no. 2, pp. 62–69, Apr. 2019.

[3] R. T. Schwarz, T. Delamotte, K.-U. Storek, and A. Knopp, "MIMO applications for multibeam satellites," *IEEE Trans. Broadcast.*, vol. 65, no. 4, pp. 664–681, Dec. 2019.

[4] M. Á. Vázquez, A. Pérez-Neira, D. Christopoulos, S. Chatzinotas, B. Ottersten, P.-D. Arapoglou, A. Ginesi, and G. Taricco, "Precoding in multibeam satellite communications: Present and future challenges," *IEEE Wireless Commun.*, vol. 23, no. 6, pp. 88–95, Dec. 2016.

[5] L. You, A. Liu, W. Wang, and X. Gao, "Outage constrained robust multigroup multicast beamforming for multi-beam satellite communication systems," *IEEE Wireless Commun. Lett.*, vol. 8, no. 2, pp. 352–355, Apr. 2019.

[6] N. Letzepis and A. J. Grant, "Capacity of the multiple spot beam satellite channel with Rician fading," *IEEE Trans. Inf. Theory*, vol. 54, no. 11, pp. 5210–5222, Nov. 2008.

[7] W. Wang, A. Liu, Q. Zhang, L. You, X. Gao, and G. Zheng, "Robust multigroup multicast transmission for frame-based multi-beam satellite systems," *IEEE Access*, vol. 6, pp. 46074–46083, 2018.

[8] L. You, K.-X. Li, J. Wang, X. Gao, X.-G. Xia, and B. Ottersten, "Massive MIMO transmission for LEO satellite communications," *IEEE J. Sel. Areas Commun.*, vol. 38, no. 8, pp. 1851–1865, Aug. 2020.

[9] Y. Zhang, Y. Wu, A. Liu, X. Xia, T. Pan, and X. Liu, "Deep learning-based channel prediction for LEO satellite massive MIMO communication system," *IEEE Wireless Commun. Lett.*, vol. 10, no. 8, pp. 1835–1839, Aug. 2021, doi: 10.1109/LWC.2021.3083267.

[10] IMT-2020 (5G) Promotion Group, "5G vision and requirements," White Paper, May 2014.

[11] L. Dai, B. Wang, Y. Yuan, S. Han, I. Chih-Lin, and Z. Wang, "Non-orthogonal multiple access for 5G: Solutions, challenges, opportunities, and future research trends," *IEEE Commun. Mag.*, vol. 53, no. 9, pp. 74–81, Sep. 2015.

[12] Y. Saito, Y. Kishiyama, A. Benjebbour, T. Nakamura, A. Li, and K. Higuchi, "Non-orthogonal multiple access (NOMA) for cellular future radio access," in *Proc. IEEE 77th Veh. Technol. Conf. (VTC Spring)*, Jun. 2013, pp. 1–5.

[13] H. Nikopour and H. Baligh, "Sparse code multiple access," in *Proc. IEEE 24th Annu. Int. Symp. Pers., Indoor, Mobile Radio Commun. (PIMRC)*, Sep. 2013, pp. 332–336.

[14] Z. Ding and H. V. Poor, "A simple design of IRS-NOMA transmission," *IEEE Commun. Lett.*, vol. 24, no. 5, pp. 1119–1123, May 2020.

[15] G. Gui, H. Huang, Y. Song, and H. Sari, "Deep learning for an effective nonorthogonal multiple access scheme," *IEEE Trans. Veh. Technol.*, vol. 67, no. 9, pp. 8440–8450, Sep. 2018.

[16] N. Ye, X. Li, H. Yu, L. Zhao, W. Liu, and X. Hou, "DeepNOMA: A unified framework for NOMA using deep multi-task learning," *IEEE Trans. Wireless Commun.*, vol. 19, no. 4, pp. 2208–2225, Apr. 2020.

[17] X. Liu, X. B. Zhai, W. Lu, and C. Wu, "QoS-guarantee resource allocation for multibeam satellite industrial Internet of Things with NOMA," *IEEE Trans. Ind. Informat.*, vol. 17, no. 3, pp. 2052–2061, Mar. 2021.

[18] C. Chen, W.-D. Zhong, H. Yang, and P. Du, "On the performance of MIMO-NOMA-based visible light communication systems," *IEEE Photon. Technol. Lett.*, vol. 30, no. 4, pp. 307–310, Feb. 15, 2018.

[19] R. Ge, D. Bian, J. Cheng, K. An, J. Hu, and G. Li, "Joint user pairing and power allocation for NOMA-based GEO and LEO satellite network," *IEEE Access*, vol. 9, pp. 93255–93266, 2021.

[20] Z. Gao, A. Liu, C. Han, and X. Liang, "Sum rate maximization of massive MIMO NOMA in LEO satellite communication system," *IEEE Wireless Commun. Lett.*, vol. 10, no. 8, pp. 1667–1671, Aug. 2021.

[21] J. H. Lee, Y. Kim, and J. Y. Ryu, "Random beam-based non-orthogonal multiple access for low latency K-user MISO broadcast channels," *Sensors*, vol. 21, no. 13, pp. 1–12, Jun. 2021.

[22] M. Sharif and B. Hassibi, "On the capacity of MIMO BC channel with partial side information," *IEEE Trans. Inf. Theory*, vol. 51, no. 2, pp. 506–522, Feb. 2005.

[23] F. Saggese, M. Moretti, and A. Abrardo, "A quasi-optimal clustering algorithm for MIMO-NOMA downlink systems," *IEEE Wireless Commun. Lett.*, vol. 9, no. 2, pp. 152–156, Feb. 2020.

JUNG HOON LEE (Member, IEEE) received the B.S. and M.S. degrees in electrical communications engineering and the Ph.D. degree in electrical engineering from the Korea Advanced Institute of Science and Technology (KAIST), Daejeon, South Korea, in 2006, 2008, and 2013, respectively. He was a Postdoctoral Research Scholar with KAIST, from September 2013 to April 2014, and a Postdoctoral Research Scholar with North Carolina State University, Raleigh, NC, USA, from August 2014 to August 2015. From September 2015 to August 2016, he was an Assistant Professor with the Department of Electronic Engineering, Jeju National University, Jeju, South Korea. He is currently an Associate Professor with the Department of Electronics Engineering, Hankuk University of Foreign Studies, Yongin, South Korea. His research interests include interference management, limited feedback, machine learning, and signal processing in communication theory and information theory.

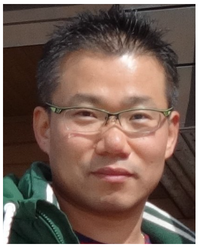

JUNG SUK JOO received the B.S., M.S., and Ph.D. degrees in electrical engineering from the Korea Advanced Institute of Science and Technology (KAIST), Daejeon, South Korea, in 1994, 1996, and 2001, respectively. From February 2001 to February 2003, he was with Samsung Electronics Company Ltd., where he was involved in the field of IMT-2000 system development. In 2003, he joined as the Faculty Member of the Hankuk University of Foreign Studies, Yongin, South Korea, where he is currently a Professor with the Department of Electronics Engineering. His research interests include adaptive signal processing and wireless communication systems.

PANSOO KIM received the B.S. and M.S. degrees in electrical and computer engineering from Sungkyunkwan University, South Korea, in 2000 and 2002, respectively. Since 2002, he has been with the Electronics and Telecommunications Research Institute (ETRI) as a Principal Researcher. His research interests include transmission technologies related with satellite communication and telecommunication systems.

JOON-GYU RYU received the B.S., M.S., and Ph.D. degrees in radio and information communications engineering from Chungnam National University, Daejeon, South Korea, in 1999, 2001, and 2014, respectively. Since 2001, he has been with the Electronics and Telecommunications Research Institute (ETRI), Daejeon, as a Principal Researcher. His research interests include satellite broadcasting and communication systems and RF technology.